EFFECTIVENESS OF HIGH-PERFORMANCE CONCRETE IN RESISTING CHLORIDE ION PENETRATION AND REINFORCEMENT CORROSION

Jon A. Jonsson, Ph.D., MACTEC Engineering and Consulting, Atlanta, GA
Jan Olek, Ph.D., P.E., Purdue University, West Lafayette, IN
Mark E. Leeman, P.E., Facility Engineering Associates, Fairfax, VA
Youlanda K. Belew, Indiana Department of Transportation, Indianapolis, IN

ABSTRACT

Premature deterioration of concrete bridges in the United States has been identified as a major problem with respect to cost of repair and rehabilitation. Most often, chloride ion penetration and subsequent corrosion of the reinforcement is the cause. Many studies have been conducted to develop concrete mixtures that will better protect the reinforcement from corroding. However, due to variability in concrete materials from one location to another, a universal solution cannot be developed. Unique approaches, each intended for a particular geographical area, are therefore needed to ensure full compatibility between locally available materials.

As a part of Indiana's high-performance concrete (HPC) bridge project, specimens from three HPC concrete mixtures and one conventional mixture were prepared and tested. The focus of the testing was to compare the ability of the four different mixtures to resist chloride ion penetration and reinforcement corrosion. Three sets of corrosion specimens were prepared from each mixture and the effective chloride ion diffusion coefficient was determined by two different test methods. These methods were chloride ponding and electrical indication of concrete's ability to resist chloride ion penetration. Correlation between results from the two test methods used to access concrete's ability to resist chloride ion ingress was good. The results presented in this paper include one-year corrosion data.

Keywords: High-Performance Concrete, Corrosion, Chlorides, Curing, Diffusion Coefficient

INTRODUCTION

In portland cement concrete, the pH of the pore solution can be expected to range from approximately 12.5 to 14 depending on the original binder composition. Reinforcing steel, when not in contact with chloride ions, will develop and maintain a passive oxide layer when exposed to solutions with a pH greater than about 11.5. The passive layer acts as a protective film and prevents corrosion of the reinforcement as long as it remains intact.

There are primarily two factors that negatively affect the stability of the passive layer of steel reinforcement embedded in concrete: carbonation and chloride ions. When carbon dioxide (CO_2) from the atmosphere diffuses into concrete, it will, in the presence of moisture, cause reactions that eventually modify the calcium hydroxide (CH) present in the hydrated cement paste. These reactions are known as carbonation process. As the CH carbonates, the pH of the pore solution decreases and eventually reaches a value of 8.3 when all the CH is carbonated.[1] At this low value of pH, the protective passive layer becomes unstable and the corrosion process can begin if adequate amounts of moisture and oxygen are present.

In 1995, Gjørv[2] concluded that carbonation was not an issue for concretes with or without silica fume when the compressive strength of the concrete was above 50 MPa (7.3 ksi). This is believed to be attributable to the high quality of the concrete microstructure when the compressive strength reaches this limit. Therefore, the focus of this paper will be confined to chloride penetration and subsequent reinforcement corrosion.

Generally, the penetration of chloride ions into concrete is considered to take place through diffusion. Ionic diffusion takes place when there is a concentration gradient and it is thought to follow Fick's 2nd law:

$$\frac{\partial \mathrm{C}}{\partial \mathrm{t}} = \frac{\partial}{\partial x}\left(D \frac{\partial \mathrm{C}}{\partial \mathrm{x}} \right) \qquad \textbf{Equation 1}$$

If the boundary conditions are assumed constant and independent of time (t), chloride content (C), and the distance (x), the solution of Fick's 2nd law becomes[3]:

$$C(x,t) = C_i + (C_s - C_i) \cdot erfc\left(\frac{x}{2\sqrt{(t - t_{ex}) \cdot D_{eff}}} \right) \qquad \textbf{Equation 2}$$

where $C(x,t)$ = chloride concentration at a given location and time
C_i = initial chloride concentration of the concrete
C_s = surface chloride concentration of the concrete
x = distance from the concrete surface
t = time from concrete placement
t_{ex} = time from concrete placement until chloride exposure
D_{eff} = effective chloride ion diffusion coefficient
$erfc(z)$ = error function complement ($erfc(z) = 1 - erf(z)$)

The units for the chloride concentrations in Equation 2 are typically in mass/volume of concrete, or as percentages of the cement content (by mass). The effective chloride ion diffusion coefficient is in units of distance squared over time, most commonly m^2/s. The distance and time factors need to be in units corresponding with the units of the diffusion coefficient.

When the chloride ion concentration in the pore solution reaches a certain threshold level, the chlorides can damage or even destroy the passive layer at pH levels well above 11.5. The threshold concentration is not a constant value, but appears to be a function of the pH.[4] Typical threshold concentration values have been considered to range from 0.9 to 1.2 kg/m^3 (1.5 to 2.0 lb/yd^3).[4]

The effective chloride ion diffusion coefficient can be determined from chloride concentrations obtained after conducting a ponding test such as AASHTO T 259. Alternatively, the electrical indication of the concrete's ability to resist chloride ion penetration (ASTM C 1202) can be determined and the value for the charge passed during the six hour test used to approximate D_{eff} based on the following equation proposed by Berke and Hicks[5]:

$$D_{eff} = 0.0103 \cdot 10^{-12} (\text{Charge Passed - coulomb})^{0.84} \qquad \textbf{Equation 3}$$

where the unit for D_{eff} is m^2/s.

EXPERIMENTAL

Three high-performance concrete (HPC) mixtures and one control mixture, meeting the requiremets of the Indiana Department of Transportation (INDOT) for Class C concrete, were batched at a ready-mix plant and then mixed and delivered by front-discharge ready-mix trucks. The minimum requirements for Class C concrete include a cement content of 390 kg/m^3 (658 lb/yd^3) and a maximum water-cement ratio of 0.443. The coarse aggregate was crushed dolomite with a maximum aggregate size of 25 mm (1 in.) and the fine aggregate was natural river sand. All of the mixtures contained the same Type I cement. Two of the HPC mixtures contained 6.5 and 8 % silica fume (SF) while the third HPC mixture contained 5 % silica fume and 30 % ground granulated blast furnace slag (GGBFS). Slump, density, and air content were measured when the trucks arrived at the testing site. Chemical analyses of the cementitious materials are given in Table 1 and mixture proportions and fresh concrete properties of the four mixtures are listed in Table 2.

From each of the four field trial mixtures, six beams were made in accordance with a modified ASTM G 109 standard (Standard Test Method for Determining the Effects of Chemical Admixtures on the Corrosion of Embedded Steel Reinforcement in Concrete Exposed to Chloride Environments). In additon, a series of five sets of steel bars, identical to those used in the G 109 beams, were assembled and placed in a 610 x 914 x 152 mm (24 x 36 x 6 in.) slab. Three of the beam specimens were moist cured for three days and the other three, along with the slab, were moist cured for 14

days. The modification of the ASTM G 109 standard included alteration of the mixture design, steel bar preparation, and salt solution concentration. The concentration of the sodium chloride solution was 6 % at the beginning of each ponding cycle.

Table 1. Chemical analyses of the cement, silica fume, and ground granulated blast furnace slag.

	Type I Cement	Silica fume	GGBFS
Chemical analyses by mass (%)			
Silicon dioxide (SiO_2)	20.16	93.07	37.73
Aluminum oxide (Al_2O_3)	4.87	0.62	7.75
Ferric oxide (Fe_2O_3)	2.92	0.41	0.39
Calcium oxide (CaO)	64.55	0.66	39.45
Magnesium oxide (MgO)	2.43	1.16	10.77
Sodium oxide (Na_2O)	0.28	0.16	0.35
Potassium oxide (K_2O)	0.09	0.79	0.29
Sulfur trioxide (SO_3)	2.55	<0.01	2.59
Titanium dioxide (TiO_2)	0.46	<0.01	0.84
Phosphorus pentoxide (P_2O_5)	0.07	0.10	<0.01
Manganic oxide (Mn_2O_3)	0.05	0.06	0.50
Strontium oxice (SrO)	0.06	<0.01	0.04
Chromic oxide (Cr_2O_3)	0.02	0.02	<0.01
Zinc oxide (ZnO)	0.03	0.10	<0.01
Loss on ignition (950°C)	1.45	2.71	-0.82
Total	99.99	99.85	99.89
Alkalies as Na_2O	0.34	0.67	0.55
Calculated potential compounds as per ASTM C 150-00 (%)			
Tricalcium silicate (C_3S)	65		
Dicalcium silicate (C_2S)	8		
Tricalcium aluminate (C_3A)	8		
Tetracalcium aluminoferrite (C_4AF)	9		

Table 2. Mixture proportions and fresh concrete properties.

Mixture ID	F-1 (Control)	F-2	F-3	F-4
(%C-%S-%SF)	100C	93.5C-6.5SF	65C-30S-5SF	92C-8SF
Cement (kg/m^3 (lb/yd^3))	389 (655)	403 (680)	279 (470)	395 (665)
Silica fume (kg/m^3 (lb/yd^3))		28 (47)	21 (36)	34 (58)
GGBFS (kg/m^3 (lb/yd^3))			129 (218)	
Total binder cont. (kg/m^3 (lb/yd^3))	389 (655)	431 (727)	430 (724)	429 (723)
Water (kg/m^3 (lb/yd^3))	154 (260)	154 (259)	165 (277)	159 (268)
Water-binder ratio	0.397	0.356	0.383	0.370
Coarse agg. (kg/m^3 (lb/yd^3))	1026 (1730)	1026 (1730)	1020 (1720)	1020 (1720)
Fine agg. (kg/m^3 (lb/yd^3))	736 (1240)	694 (1170)	659 (1110)	664 (1120)
HRWR (mL/L (oz/cwt))		593 (9.1)	619 (9.5)	828 (12.7)
NRWR/Ret. (mL/L (oz/cwt))	130 (2.0)	196 (3.0)	196 (3.0)	196 (3.0)
AEA (mL/L (oz/cwt))	85 (1.30)	173 (2.65)	231 (3.54)	194 (2.97)
Slump (mm (in.))	140 (5.5)	203 (8)	191 (7.5)	140 (5.5)
Air content (%)	6.6	6.6	7.0	8.0
Density (kg/m^3 (lb/yd^3))	2323 (145.0)	2299 (143.5)	2287 (142.8)	2297 (143.4)

The design of the series of five sets of steel bars placed in the slab was based on the ASTM G 109 configuration and corrosion sensors, designed by Schiessl and Raupach[6], where the cover of the anodic steel was varied. For this series, the cover of the anodic bars ranged from 13 mm to 64 mm (1/2 in. to 2 1/2 in.) while the cathodic bars were kept at a constant distance of 51 mm (2 in.) from their respective anodic bars. The cover of the anodic bars of the standard G 109 beams was 25 mm (1 in.).

The five sets of steel bars were supported with two small sheets of plexiglas with a thickness of 3.175 mm (0.125 in.). A photograph of a series of five sets of steel bars designed to have a variable cover thickness is shown in Figure 1. In this paper, the sets of steel bars having variable cover thickness will be referred to as ladder macrocells.

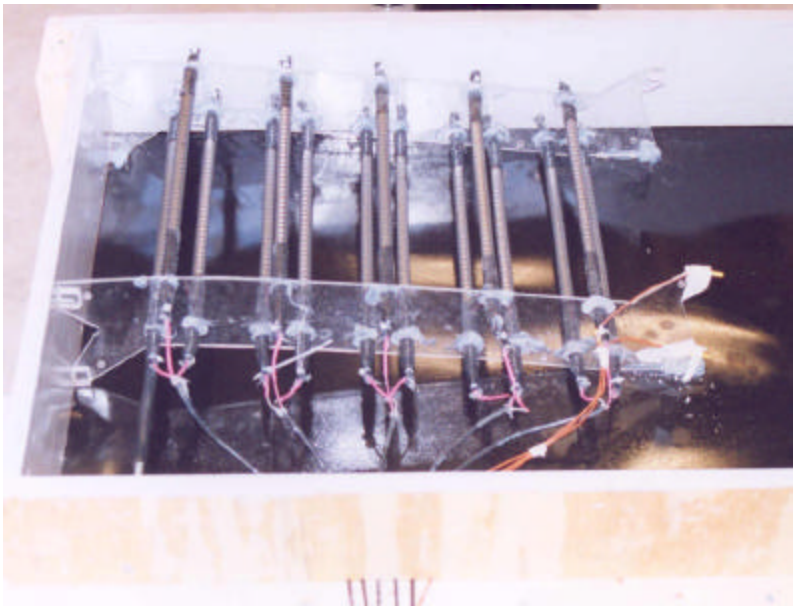

Figure 1. A series of five sets of steel bars (ladder macrocells) designed to have a variable cover thickness.

As mentioned previously, the concentration of the sodium chloride solution used to pond the specimens was 6 %. Exposure to the solution was started when the specimens were 42 days old. After four days of exposure, the solution was removed and the specimens dried under halogen heat lamps. None of the specimens were covered during the ponding, which, due to evaporation, resulted in some increase of the solution concentration during the ponding period. All corrosion specimens from each mixture were placed in the same stainless steel pan with dimensions of 914 x 1219 x 38 mm (36 x 48 x 1.5 in.) and dried with four 500 W heat lamps for three days to complete each weekly cycle.

The purpose of using the heat lamps was to create exposure conditions similar to those used by other researchers[7,8] to accelerate the deterioration process. The distance between the lamps and the specimens was 965 mm (38 in.). The lamps were effective in raising

the temperature of the slabs and the maximum temperature in the center of the slabs reached approximately 60 to 65ºC (140 to 149ºF) during the drying periods.

A 100-ohm resistor was used to connect the anodic bar of each macrocell to the cathodic bars. The potential over the resistors was monitored every 10 minutes with a Campbell Scientific CR10X datalogger and control unit. Two AM 416 multiplexers were connected to the datalogger to expand four of the six channels to 64. Forty-four of the channels were used for monitoring the corrosion specimens.

In addition to corrosion specimens, one slab from each mixture was prepared and subjected to exposure conditions described in AASHTO T 259. These slabs were ponded with 3 % NaCl solution for 90 days after they reached an age of 42 days. At the end of the ponding period, approximately 100 mm (4 in.) long cores were obtained from each slab. After the same exposure period, the slabs containing the ladder macrocells were also cored. The cores were allowed to dry for three weeks before being ground in 1 mm (39/1000 in.) increments to collect powder samples for chloride analysis.

HARDENED CONCRETE PROPERTIES

The compressive strength was determined by testing two 102 x 203 mm (4 x 8 in.) cylinders from each mixture at the age of 28 days. In addition, two specimens were tested for electrical indication of chloride ion penetration resistance (ASTM C 1202) at the age of 91 days. The results of those tests are listed in Table 3.

Table 3. Compressive strength and charged passed for the four mixtures.

Mixture (%C-%S-%SF)	Compressive strength		Charge passed
	(MPa)	(ksi)	(coulombs)
F-1 (100C)	45.0	6.53	6430
F-2 (93.5C-6.5SF)	56.2	8.16	1230
F-3 (65C-30S-5SF)	56.6	8.20	560
F-4 (92C-8SF)	62.3	9.03	520

CHLORIDE ION PENETRATION

Cores were obtained from eight slabs from the mixtures after 90 days of exposure to chloride solutions. Four of the slabs, one from each mixture, were ponded continuously with 3% NaCl for 90 days as per AASHTO T 259. The other four slabs were subjected to cycles consisting of four days of ponding with 6 % NaCl solution followed by three days of drying under heat lamps. In addition to the chloride profiles, baseline chloride contents were determined along with chloride contents in both fine and coarse aggregates.

Baseline chloride contents and chloride contents of both fine and coarse aggregates are listed in Table 4. The aggregates, particularly the coarse aggregates, appeared to be the source of the baseline chlorides.

Table 4. Baseline chloride contents and chloride contents of both fine and coarse aggregate.

	Chloride concentration (kg/m^3)	Chloride concentration (lb/yd^3)
F-1 (100C)	1.02	1.73
F-2 (93.5C-6.5SF)	1.08	1.82
F-3 (65C-30S-5SF)	1.12	1.89
F-4 (92C-8SF)	0.85	1.43
Fine aggregate	0.47	0.79
Coarse aggregate	1.53	2.58

Chloride profiles along with curves fitted to the profiles for specimens subjected to the 3 % NaCl solution are shown in Figure 2. Using Equation 2, the curves were fitted to the profiles assuming a constant surface chloride concentration of 18 kg/m^3 (30.3 lb/yd^3) and variable effective chloride ion diffusion coefficients. Mixture F-1 had the highest diffusion coefficient, or $10 \cdot 10^{-12}$ m^2/s. For mixture F-2, the diffusion coefficient was found to be $4 \cdot 10^{-12}$ m^2/s and $2 \cdot 10^{-12}$ m^2/s for mixtures F-3 and F-4.

As the temperature of the ponding slabs was higher than would normally be expected during ponding tests, the effective chloride ion diffusion coefficients for the curves shown in Figure 2 can be expected to be higher also. Based on estimates given by Bentur et al.[4], diffusion coefficients can be expected to change by roughly a factor of two for each 9°C (16°F). Analysis of the temperature data collected for the slabs revealed an average weekly temperature of 27.2°C (81.0°F). This was 4.2°C (7.6°F) higher than recommended in the standard test procedure of AASHTO T 259 and the diffusion coefficients can therefore be expected to be approximately 1.5 times higher than they would have been at the standard temperature.

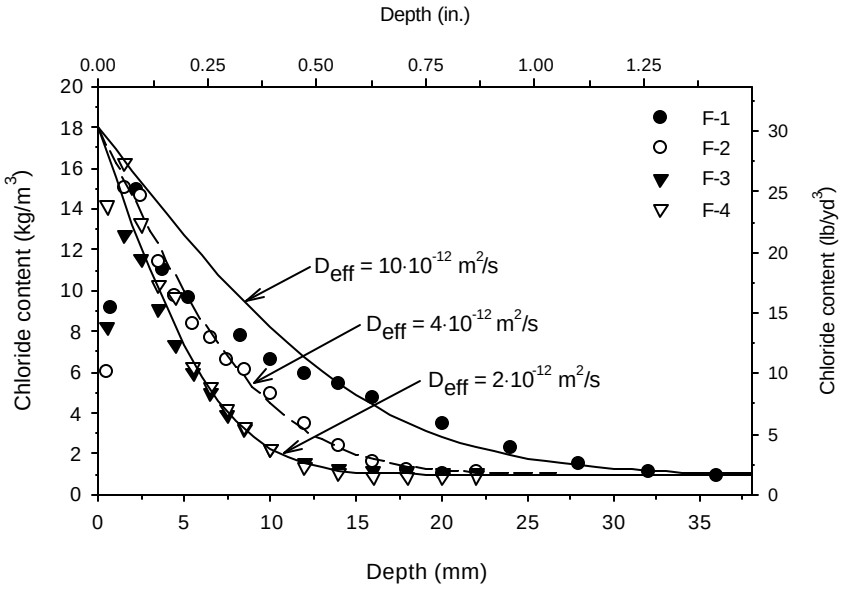

Figure 2. Chloride profiles of cores extracted from slabs ponded with 3 % NaCl solution for 90 days as described AASHTO T259. The curves were determined by using a fixed surface chloride concentration of 18 kg/m^3 (30.3 lb/yd^3) and variable diffusion coefficients as shown.

Chloride profiles for the four slabs that were subjected to cycles consisting of four days of ponding with 6 % NaCl solution followed by three days of drying under heat lamps are shown in Figure 3. The results from these specimens are not as consistent as those shown in Figure 2 as the chloride ingress may have been caused by a combination of diffusion and absorption. Good fits between the data and curves based on diffusion alone were not attained for the results shown in Figure 3. However, the relative performance of the mixtures was comparable to that observed for the slabs subjected to constant ponding of 3 % NaCl solution with the exception of results from mixture F-3 which had elevated levels of chlorides in the top 12 mm (0.5 in.).

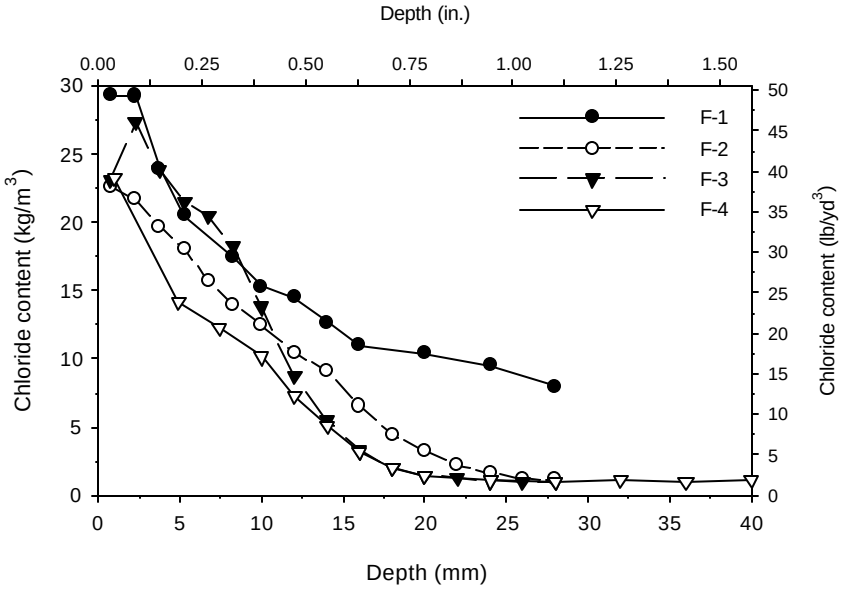

Figure 3. Chloride profiles of cores extracted from slabs subjected to weekly cycles of ponding and drying for 90 days. The ponding solution contained 6 % NaCl at the start of each ponding cycle.

CORROSION

The corrosion measurements included continuous monitoring of the potential across 100 ohm resistors connecting the anodic and cathodic bars of each macrocell. Half-cell potentials were determined manually using a copper-copper sulfate reference electrode and a high impedance digital multimeter. The half-cell measurements were performed at the end of each ponding cycle for the first six months of the testing program.

After one year of weekly cycles, the results of the corrosion measurements were only partially conclusive as only some of the macrocells exhibited corrosion activity. Corrosion currents for all macrocells from mixtures F-1 and F-2 are shown in Figures 4 to 7. Corrosion currents for macrocells from mixtures F-3 and F-4 are not included as corrosion activity was limited to the ladder macrocells with the 13 mm (0.5 in.) cover. None of the other macrocells from those two mixtures showed any indication of corrosion after 52 cycles of ponding and drying.

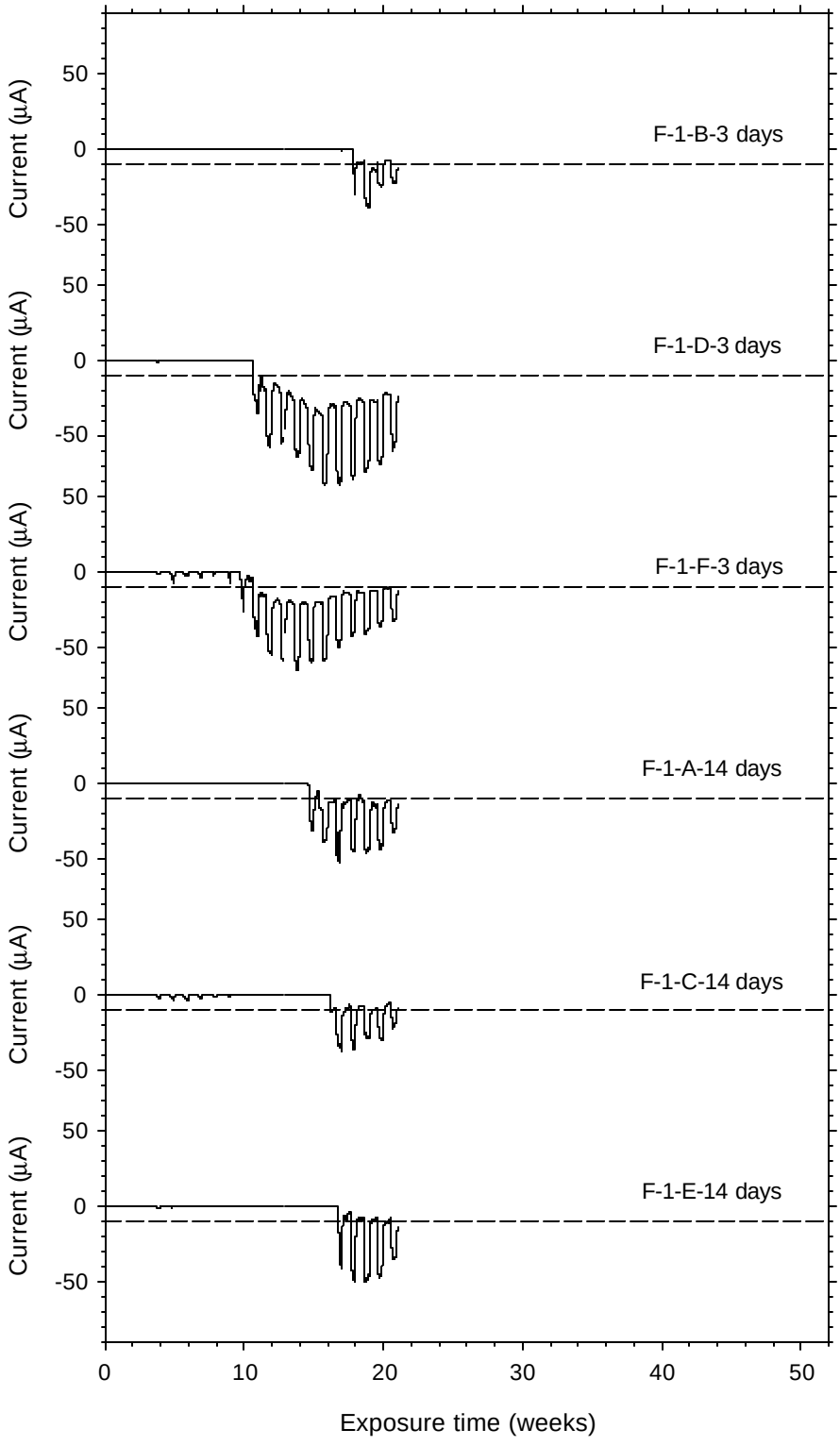

Figure 4. Corrosion currents for ASTM G 109 macrocells from mixture F-1 (100C).

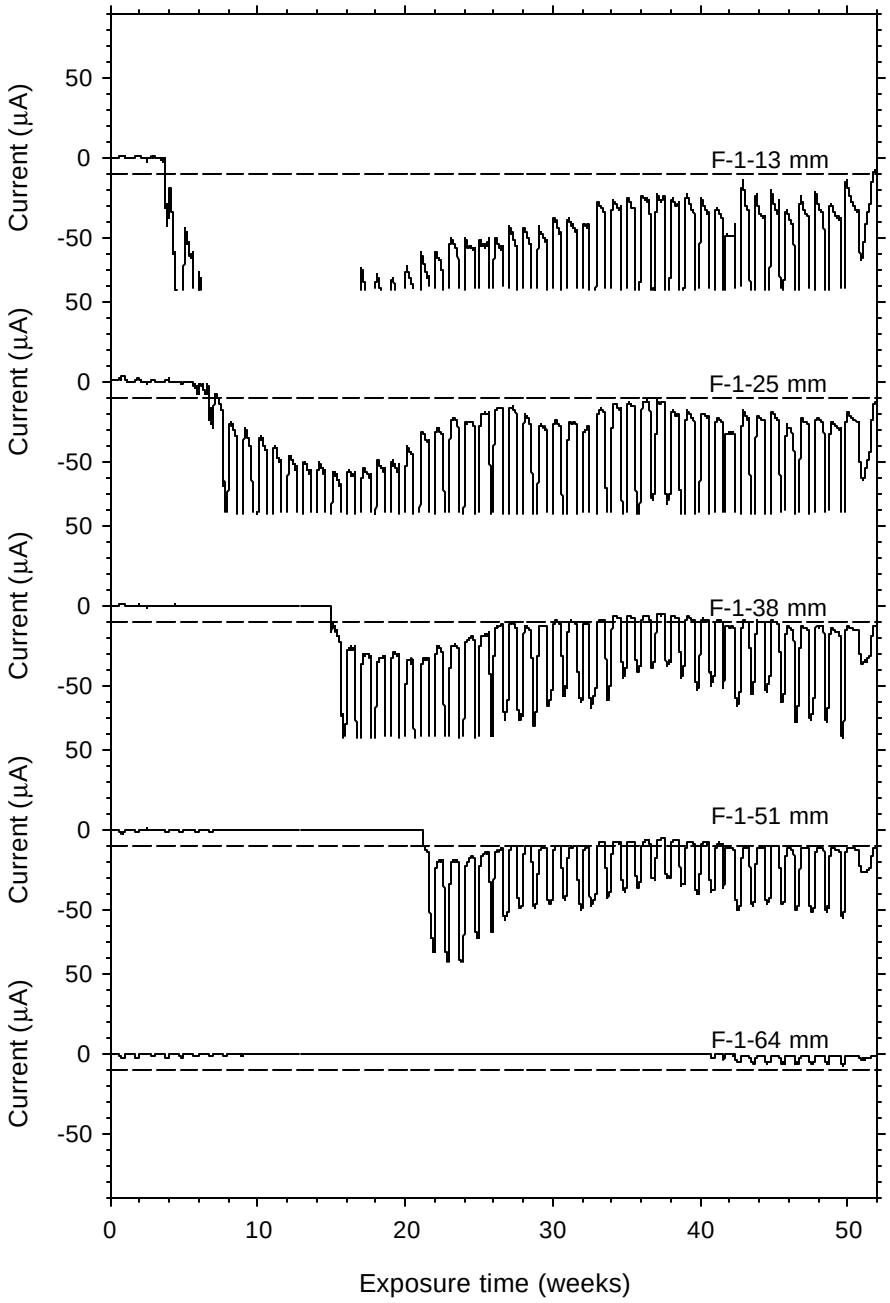

Figure 5. Corrosion currents for ladder macrocells from mixture F-1 (100C).

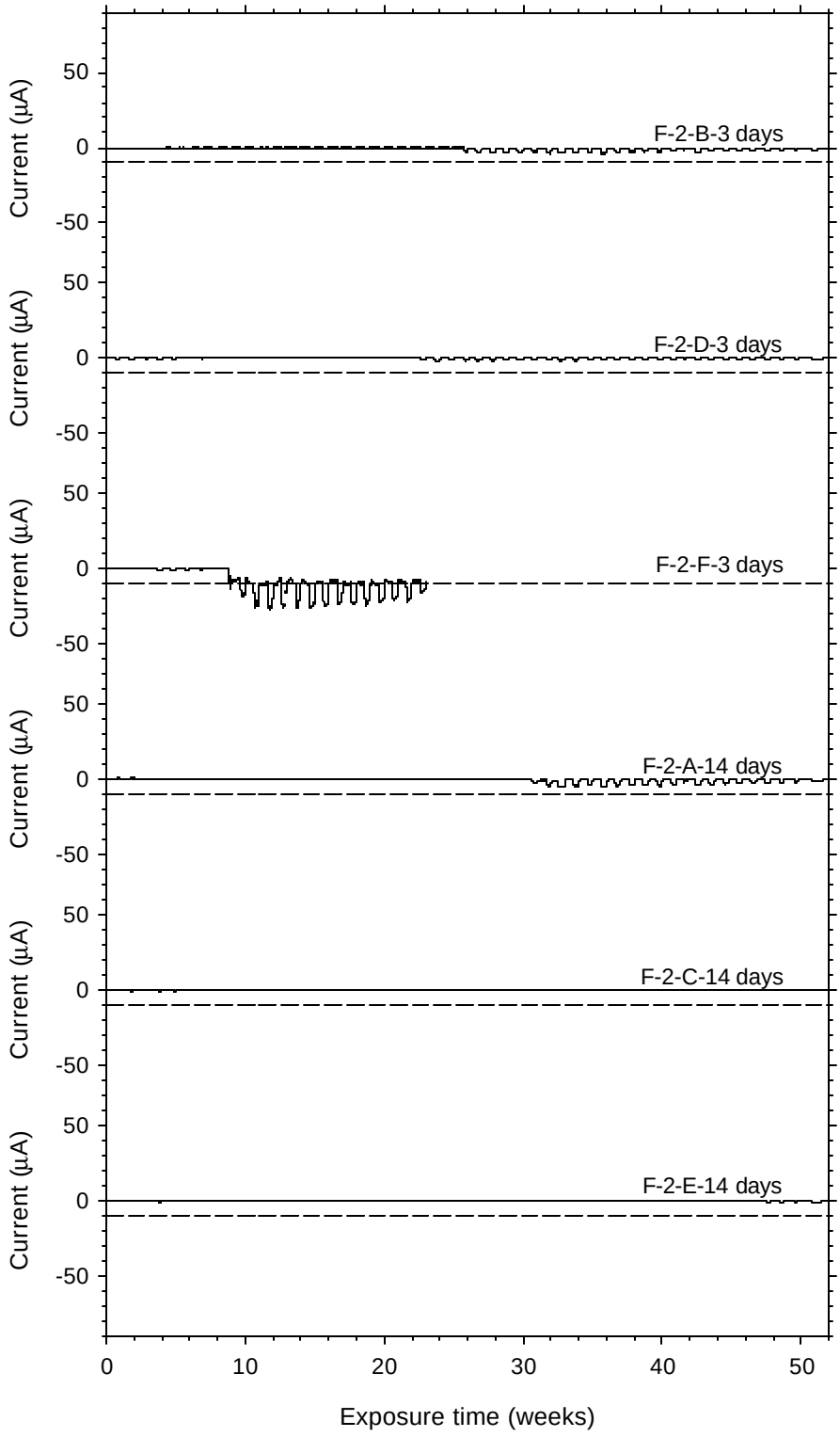

Figure 6. Corrosion currents for ASTM G 109 macrocells from mixture F-2 (93.5C-6.5SF).

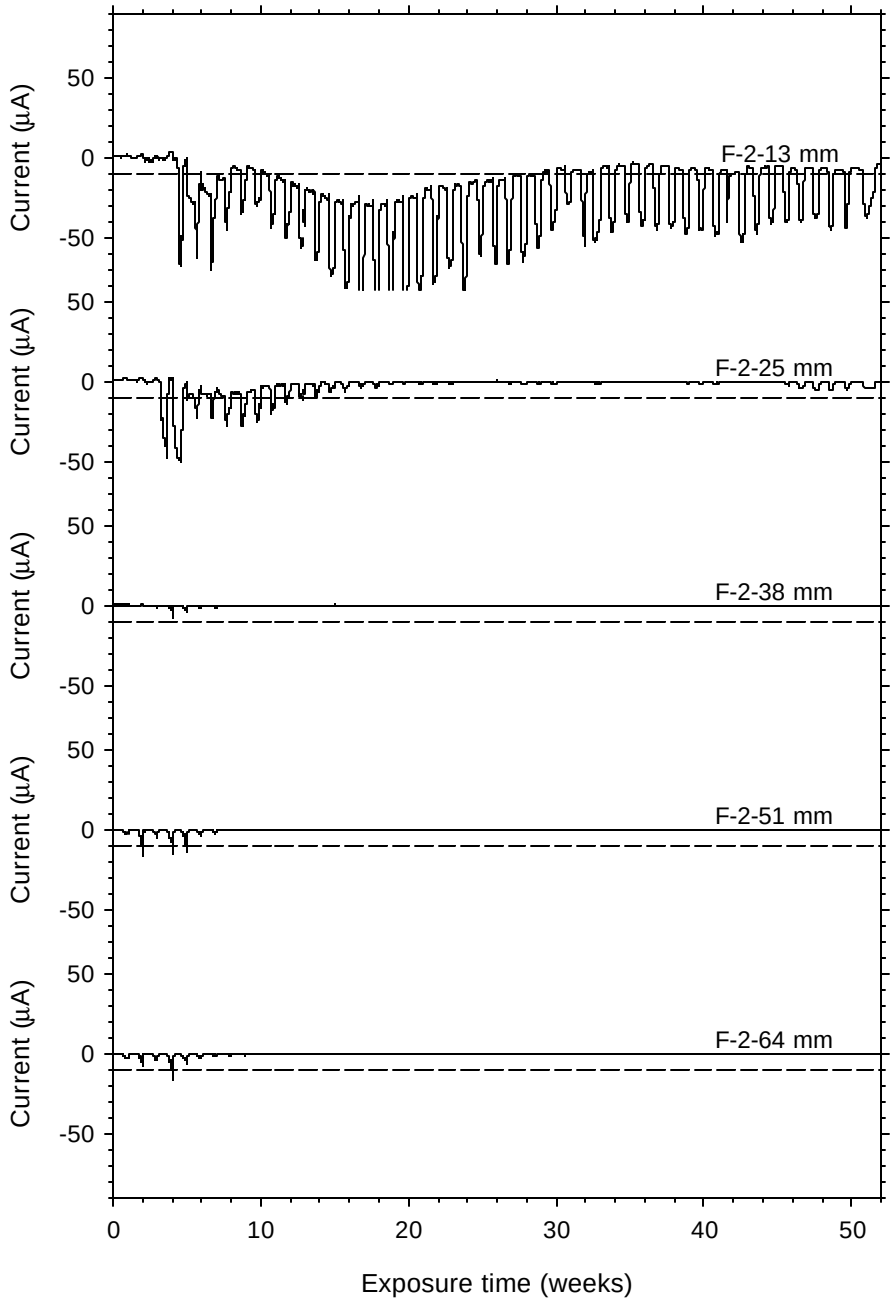

Figure 7. Corrosion currents for ladder macrocells from mixture F-2 (93.5C-6.5SF).

The analysis of the corrosion currents for the ladder macrocells were complicated by unanticipated cracking of the slabs during the initial drying periods. These cracks propagated directly above the plexiglas used to support the steel. The extent of cracking was similar for all four slabs. Although the cracks formed outside the area of exposed steel, corrosion was detected on several of the ladder macrocells during the first few weeks. High concrete temperature during the drying periods and differences in the coefficient of thermal expansion for the plexiglas and the concrete were identified as causes for the cracking.

After the cracks were identified, partitions were installed on the ponding slabs containing the ladder macrocells. The partitions were installed to prevent salt solution from entering the cracks above the plexiglas supports. This in turn gradually reduced corrosion activity of the ladder macrocells until diffusing chloride ions reached the anodic bars.

The time to corrosion of the ASTM G 109 macrocells varied considerably between the different mixtures with macrocells from F-1 (control) experiencing corrosion after less than four months. The time to corrosion for all of the macrocells is listed in Table 5. The time to corrosion was defined as the time until there was a repeated change in the corrosion current during the ponding cycles. As this happened early in the test program for specimens from F-1, the monitoring of those specimens was terminated after the average corrosion current had gone below -10 µA.

Table 5. Time to corrosion for ASTM G 109 macrocells.

Specimen	Time to corrosion (weeks)			
	F-1 (100C)	**F-2 (93.5C-6.5SF)**	**F-3 (65C-30S-5SF)**	**F-4 (92C-8SF)**
B – 3 days	18	26	52^+	52^+
D – 3 days	11	23	52^+	52^+
F – 3 days	10	9*	52^+	52^+
Avg. – 3 days	**13**	**25**	**52^+**	**52^+**
A – 14 days	15	31	52^+	52^+
C – 14 days	16	52^+	52^+	52^+
E – 14 days	17	48	52^+	52^+
Avg. – 14 days	**16**	**44^+**	**52^+**	**52^+**

***** Value not included in average as specimen was assumed to have been defective.
$^+$ Indicates the final value will be higher.

The results of the half-cell measurements correlated well with the results of the corrosion current monitoring. Measured half-cell potentials of less than -350 mV generally coincided with corrosion currents of less than -10 µA. In ASTM G 109, the time to failure is defined as the time required for the average macrocell current to reach a magnitude of 10 µA. The dashed lines in Figures 4 to 7 drawn at -10 µA act as a guide in determining the time to failure of the individual corrosion specimens.

DISCUSSION

The baseline chloride contents were higher than anticipated, as they were approximately equal to the typical threshold level for corrosion of 0.9 to 1.2 kg/m^3 (1.5 to 2.0 lb/yd^3).[4] In another study, where similar raw materials were used, average baseline chloride ion concentrations of 0.85 kg/m^3 (1.43 lb/yd^3) were found.[7] In this study, the aggregates, particularly the crushed dolomite coarse aggregate, were the main source of baseline chlorides. Determining the stability of the chlorides within the aggregates may be of interest as they are likely to reduce the time to corrosion if they diffuse from the aggregates into the cement paste.

The correlation between the three methods used in this research program to evaluate the effectiveness of HPC in resisting chloride ion penetration and reinforcement corrosion appears good. In particular, the values for D_{eff} obtained from the ponding tests and Equation 3, listed in Table 6, showed good correlation. Although the corrosion experiments were only partially conclusive after one year of exposure to chloride solution, the relative performance of the different mixtures could have been predicted at the start of the testing based on the D_{eff} values.

Table 6. Diffusion coefficients obtained from Figure 2 and calculated from Equation 3.

Mixture	Diffusion coefficients from Figure 2 (10^{-12} m^2/s)	Diffusion coefficients from Equation 3 (10^{-12} m^2/s)
F-1 (100C)	10	16.3
F-2 (93.5C-6.5SF)	4	4.05
F-3 (65C-30S-5SF)	2	2.09
F-4 (92C-8SF)	2	1.98

Based on the estimated diffusion coefficients, the time to corrosion of reinforcement in mixtures F-3 and F-4 can be expected to be five times longer than in mixture F-1 and two times longer than in mixture F-2. If the typical time to corrosion in bridge decks is assumed to be 15 years when INDOT Class C concrete (mixture F-1) is used, the time to corrosion of bridge decks utilizing either mixture F-3 or F-4 can be estimated to be 75 years.

For mixtures F-1 and F-2, where corrosion activity was detected for 11 out of 12 ASTM G 109 macrocells, additional moist curing after the first three days was beneficial. For F-1, the increase in average time to corrosion was three weeks, or approximately 25 %. For F-2, the corresponding values were at least 19 weeks and 75 %. Based on these results, the benefit of extended moist curing appears greater for HPC than conventional concrete.

The heat lamps were effective in raising the temperature of the concrete and facilitate drying. In fact, the internal concrete temperatures measured during the drying periods were higher than expected. Measured surface temperatures when similar set ups had been used were 49ºC (120ºF)[7] and 43ºC (110ºF)[8] while in this study the internal concrete temperature reached approximately 60 to 65ºC (140 to 149ºF). Furthermore, the concrete surface temperatures showed some variations as the amount of light/heat emitted by the lamps was variable. In terms of energy use and uniform heating conditions, a heated room or an enclosure may have been more efficient than the fluorescent lamps.

CONCLUSIONS

All of the high performance concrete mixtures tested in this study had lower chloride ion diffusion rates than INDOT's standard Class C concrete mixture. Based on the measured effective chloride ion diffusion coefficients, the time to corrosion for reinforcement placed in the high performance concrete mixtures can be expected to be up to five times longer than if the reinforcement was placed in the Class C concrete.

Estimating the effective chloride ion diffusion coefficient, D_{eff}, from values obtained from electrical indication of the concrete's chloride ion penetration resistance (ASTM C 1202) appears a valid method for assessing the anticipated resistance of the concrete to chloride ion penetration. The estimated D_{eff} values compared well with values determined from chloride profiles for slabs that had been ponded with 3 % sodium chloride solution for 90 days.

Increasing the moist curing period from three days to 14 days was effective in increasing the time to corrosion. This was evident for two of the four mixtures tested. The results for the other two mixtures were inconclusive as corrosion activity had not been detected after 52 weekly cycles of wetting and drying.

Crushed dolomite and natural sand aggregates can contribute enough chlorides to bring the baseline chloride ion concentration to levels typically considered sufficient to cause corrosion. Further research may be warranted to determine the stability of the chlorides contained in the aggregates and if they will diffuse into the paste and increase the risk of reinforcement corrosion.

ACKNOWLEDGEMENTS

The authors gratefully acknowledge the Indiana Department of Transportation and the Joint Transportation Research Project for supporting this research. The assistance of Dr. Chengqing Qi in overseeing the corrosion experiments during the last 22 weeks of testing is also much appreciated.

REFERENCES

1. Neville, A. M., *Properties of Concrete*, Fourth Edition, John Wiley & Sons, New York, 1996, 884 pp.
2. Gjørv, O. E., "Effect of Condensed Silica Fume on Steel Corrosion in Concrete," *ACI Materails Journal*, Vol. 92, No. 6, November-December 1995, pp. 591-598.
3. Poulsen, E., "Estimation of Chloride Ingress into Concrete and Prediction of Service Lifetime with Reference to Marine RC Structures," *Durability of Concrete in Saline Environment*, Cementa AB, Danderyd, Sweden, 1996, pp. 113-126.
4. Bentur, A., Diamond, S., and Berke, N. S., *Steel Corrosion of Concrete: Fundamentals and Civil Engineering Practice*, E & FN Spon, London, 1997, 201 pp.
5. Berke, N. S. and Hicks, M. C, "The Life Cycle of Reinforced Concrete Decks and Marine Piles Using Laboratory Diffusion and Corrosion Data," *Corrosion Forms and Control For Infrastructure, ASTM STP 1137,* V. Chaker, Ed., American Society for Testing and Materials, Philadelphia, PA, 1992, pp. 207-231.
6. Schiessl, P. and Raupach, M., "Monitoring System for the Corrosion Risk of Steel in Concrete Structures," *Concrete International*, Vol. 14, No. 7, 1992, pp. 52-55.

7. Samples, L. M. and Ramirez, J. A., *Methods of Corrosion Protection and Durability of Concrete Bridge Decks Reinforced with Epoxy-Coated Bars-Phase I*, Joint Transportation Research Program, Report FHWA/IN/JTRP-98/15, Purdue University, West Lafayette, IN, 1999, 258 pp.
8. Liu, R., *Development and Evaluation of Cement-based Materials for Repair of Corrosion-damaged Reinforced Concrete Slabs*, Ph.D. Thesis, Purdue University, West Lafayette, Indiana, 2000, 276 pp.